Other optical techniques for the production of photonic crystals use a tightly focused scanning laser beam to initiate chemical vapour deposition[25] or two-photon photopolymerization[26]. Structures are produced layer-by-layer, so these techniques are relatively slow; they are currently limited to micrometre length scales. Semiconductor microfabrication[27–29], which has the required resolution, is an expensive process at the limit of current technology and has not produced structures more than a few unit cells deep. Colloidal crystals may be used as templates to make submicrometre structures[14–18], but the use of close-packed spheres severely restricts the range of lattices that may be produced[30] and allows almost no freedom to alter the structure of a unit cell. By contrast, the optical properties of microstructures made by holographic lithography may be optimized by controlling the form of the interference pattern. Our fabrication method has the high spatial resolution required to produce photonic crystals for the visible spectrum, as well as creating the connected air and dielectric networks that are important for the opening of a full bandgap. The process is cheap, rapid and potentially scalable for large-scale production. We have also shown that these polymeric structures may be used as templates for the construction of photonic crystals with higher refractive-index contrast. We believe that this is an enabling technology that should allow the theoretical potential of visible optical photonic crystals to be realized. □

Received 13 September; accepted 20 December 1999.

1. Yablonovitch, E. Inhibited spontaneous emission in solid-state physics and electronics. *Phys. Rev. Lett.* **58,** 2059–2062 (1987).
2. Joannopoulos, J. D., Villeneuve, P. R. & Fan, S. Photonic crystals: putting a new twist on light. *Nature* **386,** 143–149 (1997).
3. Krauss, T. F. & De La Rue, R. M. Photonic crystals in the optical regime—past, present and future. *Prog. Quantum Electron.* **23,** 51–96 (1999).
4. Yablonovitch, E. *et al.* Donor and acceptor modes in photonic band structure. *Phys. Rev. Lett.* **67,** 3380–3383 (1991).
5. Lin, S.-Y., Chow, E., Hietala, V., Villeneuve, P. R. & Joannopoulos, J. D. Experimental demonstration of guiding and bending of electromagnetic waves in a photonic crystal. *Science* **282,** 274–276 (1998).
6. Foresi, J. S. *et al.* Photonic-bandgap microcavities in optical waveguides. *Nature* **390,** 143–145 (1997).
7. Fan, S., Villeneuve, P. R. & Joannopoulos, J. D. High extraction efficiency of spontaneous emission from slabs of photonic crystals. *Phys. Rev. Lett.* **78,** 3294–3297 (1997).
8. John, S. & Wang, J. Quantum optics of localized light in a photonic band gap. *Phys. Rev. B* **43,** 12772–12789 (1991).
9. Grynberg, G., Lounis, B., Verkerk, P., Courtois, J.-Y. & Salomon, C. Quantized motion of cold cesium atoms in two- and three-dimensional optical potentials. *Phys. Rev. Lett.* **70,** 2249–2252 (1993).
10. Yablonovitch, E., Gmitter, T. J. & Leung, K. M. Photonic band structure: the face-centred-cubic case employing nonspherical atoms. *Phys. Rev. Lett.* **67,** 2295–2298 (1991).
11. Ho, K. M., Chan, C. T. & Soukoulis, C. M. Existence of a photonic gap in periodic dielectric structures. *Phys. Rev. Lett.* **65,** 3152–3155 (1990).
12. Berger, V., Gauthier-Lafaye, O. & Costard, E. Photonic band gaps and holography. *J. Appl. Phys.* **82,** 60–64 (1997).
13. Lee, K. Y. *et al.* Micromachining applications of a high resolution ultrathick photoresist. *J. Vac. Sci. Technol. B* **13,** 3012–3016 (1995).
14. Kapitonov, A. M. *et al.* Photonic stop band in a three-dimensional SiO_2/TiO_2 lattice. *Phys. Status Solidi A* **165,** 119–123 (1998).
15. Holland, B. T., Blanford, C. F. & Stein, A. Synthesis of macroporous minerals with highly ordered three-dimensional arrays of spheroidal voids. *Science* **281,** 538–540 (1998).
16. Wijnhoven, J. E. G. J. & Vos, W. L. Preparation of photonic crystals made of air spheres in titania. *Science* **281,** 802–804 (1998).
17. Imhof, A. & Pine, D. J. Ordered macroporous materials by emulsion templating. *Nature* **389,** 948–951 (1997).
18. Zakhidov, A. A. *et al.* Carbon structures with three-dimensional periodicity at optical wavelengths. *Science* **282,** 897–901 (1998).
19. Subramanian, G., Manoharan, V. N., Thorne, J. D. & Pine, D. J. Ordered macroporous materials by colloidal assembly: a possible route to photonic bandgap materials. *Adv. Mater.* **11,** 1261–1265 (1999).
20. Mayo, M. J. Processing of nanocrystalline ceramics from ultrafine particles. *Int. Mater. Rev.* **41,** 85–115 (1996).
21. Klein, J. D. *et al.* Electrochemical fabrication of cadmium chalcogenide microdiode arrays. *Chem. Mater.* **5,** 902–904 (1993).
22. Vlasov, Y. A., Yao, N. & Norris, D. J. Synthesis of photonic crystals for optical wavelengths from semiconductor quantum dots. *Adv. Mater.* **11,** 165–169 (1999).
23. Velev, O. D., Tessier, P. M., Lenhoff, A. M. & Kaler, E. W. A class of porous metallic nanostructures. *Nature* **401,** 548 (1999).
24. Tarhan, İ. İ. & Watson, G. H. Photonic band structure of fcc colloidal crystals. *Phys. Rev. Lett.* **76,** 315–318 (1996).
25. Wanke, M. C., Lehmann, O., Müller, K., Wen, Q. Z. & Stuke, M. Laser rapid prototyping of photonic band-gap microstructures. *Science* **275,** 1284–1286 (1997).
26. Cumpston, B. H. *et al.* Two-photon polymerization initiators for three-dimensional optical data storage and microfabrication. *Nature* **398,** 51–54 (1999).
27. Cheng, C. C. *et al.* New fabrication techniques for high quality photonic crystals. *J. Vac. Sci. Technol. B* **15,** 2764–2767 (1997).
28. Noda, S., Yamamoto, N. & Sasaki, A. New realization method for three-dimensional photonic crystal in optical wavelength region. *Jpn J. Appl. Phys.* **35,** L909–L912 (1996).
29. Fleming, J. G. & Lin, S.-Y. Three-dimensional photonic crystal with a stop band from 1.35 to 1.95 μm. *Opt. Lett.* **24,** 49–51 (1999).
30. van Blaaderen, A., Ruel, R. & Wiltzius, P. Template-directed colloidal crystallization. *Nature* **385,** 321–324 (1997).

Acknowledgements

We thank A. J. Wilkinson and the Department of Materials, University of Oxford, for use of scanning electron microscope facilities. This work was supported by the EPSRC/MOD/DERA Joint Grant Scheme, under the Microstructured Photonic Materials Initiative.

Correspondence should be addressed to A.J.T. (a.turberfield@ physics.oxford.ac.uk).

Electrophoretic assembly of colloidal crystals with optically tunable micropatterns

R. C. Hayward, D. A. Saville & I. A. Aksay

Department of Chemical Engineering and Princeton Materials Institute, Princeton University, Princeton, New Jersey 08544-5263, USA

The production of materials with micrometre- and submicrometre-scale patterns is of importance in a range of applications, such as photonic materials[1,2], high-density magnetic data storage devices[3], microchip reactors[4] and biosensors[5]. One method of preparing such structures is through the assembly of colloidal particles[5–10]. Micropatterned colloidal assemblies have been produced with lithographically patterned electrodes[5,11] or micromoulds[12]. Here we describe a different method that combines the well-known photochemical sensitivity of semiconductors[13,14] with electric-field-induced assembly[15,16] to create ordered arrays of micrometre-sized colloidal particles with tunable patterns. We show that light affects the assembly processes, and demonstrate

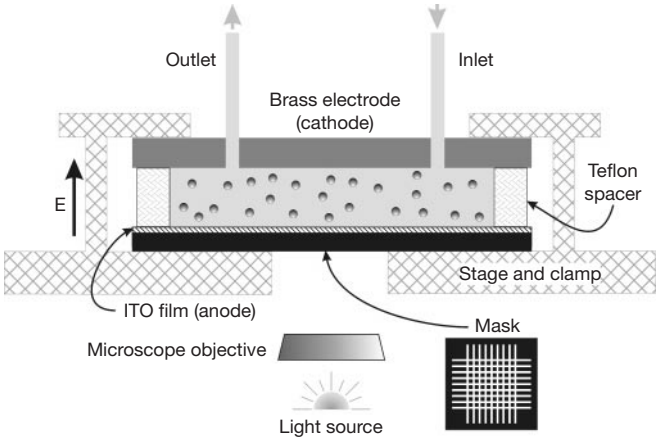

Figure 1 Schematic of the apparatus for particle assembly and pattern formation. The ITO (indium tin oxide) and brass electrodes are separated with a 500-μm Teflon spacer. When desired, the mask is positioned outside the cell between the light source and the glass electrode. Patterns are imaged using a CCD camera mounted on a Leitz Metallovert optical microscope. In most cases, 50 μl of a dilute suspension of polystyrene particles (diameter 2 μm, Duke Scientific) is used to provide a 1-cm^2 lens sandwiched between the electrodes. A positive potential is applied to the ITO electrode while the cathode is grounded; current through the cell is monitored with a multimeter.

how to produce patterns using electrophoretic deposition in the presence of an ultraviolet (UV) illumination motif. The distribution of current across an indium tin oxide (ITO) electrode can be altered by varying the illumination intensity: during the deposition process, this causes colloidal particles to be swept from darkened areas into lighted regions. Illumination also assists in immobilizing the particles on the electrode surface. Although the details of these processes are not well understood, the patterning effects of the UV light are discussed in terms of alterations in the current density[15,17] that affects particle assembly on an ITO electrode.

We demonstrated the effect of current-density modulation (produced by UV light) on the electrophoretic deposition and assembly of colloid crystals using the apparatus shown in Fig. 1. In most cases, 2-μm polystyrene particles were used; similar observations were made with submicrometre-sized silica. A d.c. electric field strength of ~6,500 V m^{-1} was used in conjunction with a broad-spectrum light source and a filter that absorbed 100% of the incident radiation at wavelengths below 495 nm. Briefly, our results were as follows. When a potential of 1.3 V was applied with the filter in place, no colloidal crystals formed. On removal of the filter, crystalline aggregates formed rapidly in the illuminated region, and the cell current increased in proportion to the lighted area. When selected regions of the ITO electrode were illuminated in this manner, particles migrated slowly into the illuminated areas. None of the effects of current-density modulation were observed when the ITO electrode was replaced by a transparent 25-Å layer of sputter-coated iridium, illustrating that a conducting electrode alone is not sufficient for the modulation of colloidal assembly by UV light.

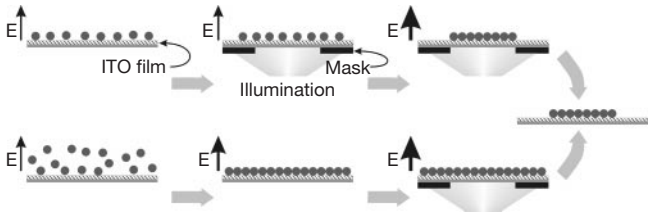

Figure 2 Process schemes for pattern formation. UV light is used to selectively assemble and affix (method A; above) or affix (method B; below) polystyrene particles on the ITO electrode. The thickness of the vertical arrows indicates the (relative) strengths of applied potentials.

We consider first the process of particle assembly. Assembling colloidal particles by the application of an electric field, a phenomenon first reported by Richetti *et al.*[18,19], is a technique for producing "crystalline" particle arrays[20,21]. Although the details of the assembly mechanism are not fully understood, the process involves simple coulombic interactions which bring particles close to an electrode surface, together with lateral motion stemming from electrohydrodynamic[15,17] or electroosmotic effects[22]. Once the particles are close to the surface, where they remain mobile, electrohydrodynamic or electrokinetic processes assemble them into arrays. Particles can be permanently attached to the surface by increasing the attractive force between the particles and the electrode[23]. When the attractive forces exceed that due to steric repulsion, entry into the "primary minimum" creates a permanent bond.

In our earlier work[15,17], we showed that altering the current density affected the motion of particles and fluid near an electrode. Moreover, it is well-known that photochemical processes alter the current at the interface between a semiconductor and an aqueous solution[13,14]. Therefore, it follows that illumination patterns could be used to modulate the assembly processes. The experiments described here demonstrate that UV light can be so used. An unusual feature of the technique is that illumination can be externally controlled. Accordingly, the assembly processes can be manipulated or "tuned" by adjusting illumination patterns (and intensity) and applied voltage level (and waveform).

We now consider how the UV light could affect the current density at the ITO electrode. The specificity of this light-effect to the ITO electrode system, and the disappearance of the effect with the introduction of a filter that absorbs light below 495 nm, suggest an interaction between UV light and the electronic band structure of ITO. ITO is a heavily doped n-type semiconductor with a bandgap between 3.5 and 4.3 eV, depending on its composition and method of preparation[24]. A UV–visible spectrum of the coated electrode used here indicates that it is opaque to light at wavelengths below 310 nm, and transmits between 70 and 90% of radiation above 400 nm. The spectrum agrees well with those reported in the literature[25,26].

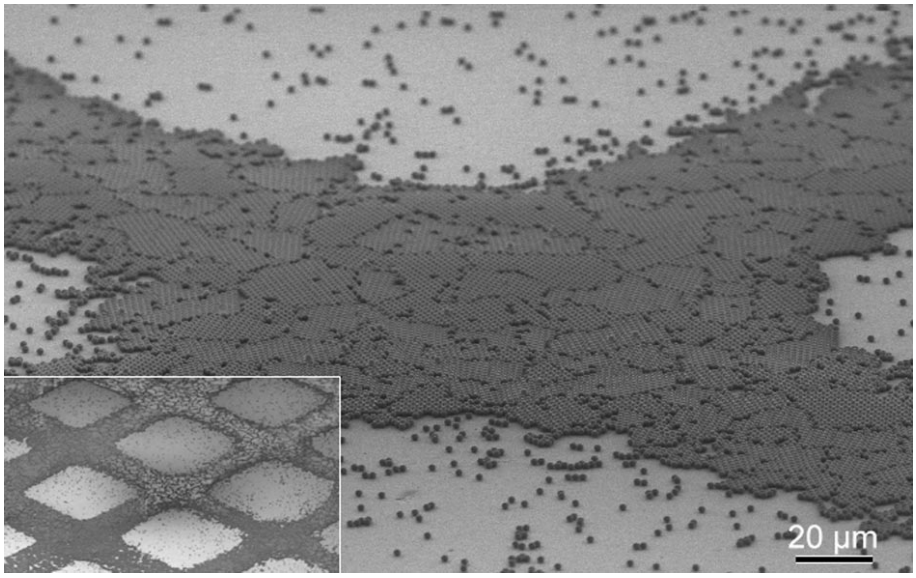

Figure 3 Scanning electron microscope image of a pattern produced by method B. Note that dense-packing of particles results in crystalline (ordered) domains that vary in size (10–20 μm). The inset (~600 μm wide) shows the overall appearance of the pattern. Some areas shown in the inset appear white due to particle charging in the SEM. Charging in these regions may result from the higher particle density which inhibits charge transfer from the uppermost particles to the conducting substrate.

Illumination of the ITO electrode by UV light results in a small increase in the measured current through the cell when a constant voltage is applied. In our experiments, only a small area was illuminated, and the overall increase in current due to illumination was only a few per cent. As Trau *et al.*[15,17] note, this current results from a redox reaction of water which forms hydrogen and oxygen at the electrodes. This conforms with the observation of gas-bubble formation in the cell at current densities greater than 100 $\mu A\ cm^{-2}$. van den Meerakker *et al.*[24] suggest that the increase in cell current on illumination with UV light is a result of the generation—at the ITO/water interface—of hole–electron pairs, and their migration. This is consistent with statements by Bocarsly *et al.*[14] that an n-type semiconductor at anodic potentials undergoes band bending at a solid–liquid interface. Electrons at the ITO surface are at a higher energy level than those in the bulk because they are surrounded by fewer metal cations[13]. When an electron–hole pair is created in this region via absorption of a photon, the promoted electron lowers its energy by moving away from the surface. Correspondingly, the new hole in the valence band moves toward the surface, where it becomes available for surface reactions. This process increases the rate of charge transfer between solution and electrode and, therefore, the current density within the cell.

As Trau *et al.*[15,17] first noted, particles are swept into regions of higher current density. Moreover, both the electrohydrodynamic[15,17] and the electroosmotic theories[22] argue that particle movement should increase with current density and with field strength. Thus, illumination of the ITO electrode with UV light should enhance particle migration because it causes an increase in current density. Correspondingly, an increased current implies a greater potential drop across the electrolyte, so the electric field in the bulk is stronger. As illumination increases the field strength, it follows that particles in illuminated regions should be more strongly attracted to the electrode surface.

We now describe the methods we used to produce patterned assemblies of colloids. Two methods were employed (Fig. 2). Both employ a lithographic mask—consisting of regularly arranged areas (~200-μm squares) of UV-absorbing ink, with ~100-μm clear areas between them—printed on a clear acetate sheet. When the mask is inserted between the ITO electrode and a light source, only selected areas of the electrode surface are illuminated by UV light.

Method A employs a suspension with a particle concentration just sufficient to produce the desired monolayer pattern. With a filter in place to cut out UV light, a d.c. voltage (1.1 V) induces deposition onto the ITO surface over a period of ~30 min. As the field strength is low, the particles retain a significant lateral mobility. The filter is then removed from the broad-band microscope light source, and the lithographic pattern is inserted to induce particle assembly in the illuminated regions. Over a period of ~2.5 h, particles in the "dark" regions are swept into the illuminated areas and the colloidal crystals grow. When the illuminated areas are filled, the strength of the electric field is increased to 3 V to irreversibly fix particles to the surface and form a permanent pattern.

In patterns fabricated by method A, most of particles are affixed to the electrode in areas illuminated by UV light. Within the illuminated regions, small crystalline domains form (generally no more than 5–10 particles across) with many gaps and imperfections. However, a substantial number of isolated particles remain in the "dark" regions of the electrode. Within the dark regions, surface coverage declines from ~50% to ~20% after 1–2 h of illumination. Continued illumination does not alter this distribution. Evidently, particle migration into illuminated regions is not strong enough to form fully dense crystals or to completely clear particles from the dark areas.

Method B employs the same apparatus with a long-wavelength UV source. Here, the initial particle concentration is just sufficient to form a monolayer over the whole surface. Particles are first attracted to the ITO anode by applying a potential of 1 V for ~30 min. Then the potential is increased to 1.5 V for 10 min to assemble particles into a dense crystalline monolayer. At this field strength, the particles are not bonded to the electrode and resuspension occurs if the potential is removed. Next, the deposit is illuminated with the long-wavelength UV light source with the lithographic mask in place, and the potential increased to 3 V for 45 min. This creates a pattern of permanently bonded particles. After disassembly, the ITO electrode is rinsed with deionized water and ethanol to remove loose particles.

Particles remaining on the electrode surface following the patterning experiments were imaged via secondary electron imaging in a scanning electron microscope (SEM). Images of a pattern constructed by method B are shown in Figure 3. The intersecting strips of particles affixed to the electrode extended over most of the 1-cm^2 area of the sample cell. Although monolayer coverage prevails in the strips, there are regions where the coverage is thicker or thinner. A smattering of single particles and small clusters are present in "empty" regions (the square holes in the pattern). The polycrystalline nature of the particle layer and the specificity of the patterning procedure are clearly evident in this image.

Although our experiments employed micrometre-sized particles of polystyrene, as well as submicrometre-sized silica, and patterns with characteristic length scales of 100 μm, the technique we report here should be applicable, within the constraints of colloidal particle size and mask length scales, to near-UV lithographic patterning. Because an external UV light source is used to modulate the particle assembly process, and the location and intensity of such a light beam can be externally controlled, the technique described here offers many possibilities for orchestrating electrophoretic deposition of optically tunable patterned arrays of small particles. □

Received 27 September; accepted 30 December 1999.

1. Lin, S. -Y., Chow, E., Hietala, V., Villeneuve, P. R. & Joannopoulos, J. D. Experimental demonstration of guiding and bending of electromagnetic waves in a photonic crystal. *Science* **282,** 274–276 (1998).
2. Painter, O. *et al.* Two-dimensional photonic band-gap defect mode laser. *Science* **284,** 1819–1821 (1999).
3. Haginoya, C., Ishibashi, M. & Koike, K. Nanostructure array fabrication with a size-controllable natural lithography. *Appl. Phys. Lett.* **71,** 2934–2936 (1997).
4. Gau, H., Herminghaus, S., Lenz, P. & Lipowsky, R. Liquid morphologies on structured surfaces: from microchannels to microchips. *Science* **283,** 46–49 (1999).
5. Velev, O. D. & Kaler, E. W. In situ assembly of colloidal particles into miniaturized biosensors. *Langmuir* **15,** 3693–3698 (1999).
6. Andres, R. P. *et al.* Research opportunities on clusters and cluster-assembled materials - a Department of Energy, Council on Materials Science panel report. *J. Mater. Res.* **4,** 704–736 (1989).
7. Inanc, I. T. & Watson, G. H. Photonic band structure of fcc colloidal crystals. *Phys. Rev. Lett.* **76,** 315–318 (1996).
8. Wijnhoven, J. E. G. J. & Vos, W. L. Preparation of photonic crystals made of air spheres in titania. *Science* **281,** 802–804 (1998).
9. Asher, S. A., Holtz, J., Weissman, J. & Pan, G. Mesoscopically periodic photonic-crystal materials for linear and nonlinear optics and chemical sensing. *MRS Bull.* **23,** 44–50 (1998).
10. Bertone, J. F., Jiang, P., Hwang, K. S., Mittleman, D. M. & Colvin, V. L. Thickness dependence of the optical properties of ordered silica-air and air-polymer photonic crystals. *Phys. Rev. Lett* **83,** 300–303 (1999).
11. Yeh, S. -R., Seul, M. & Shraiman, B. I. Assembly of ordered colloidal aggregates by electric-field-induced fluid flow. *Nature* **386,** 57–59 (1997).
12. Kim. E., Xia, Y. N. & Whitesides, G. M. Two- and three dimensional crystallization of polymeric microspheres by micromolding in capillaries. *Adv. Mater.* **8,** 245–247 (1996).
13. Morrison, S. R. *Electrochemistry at Semiconductor and Oxidized Metal Electrodes* (Plenum, New York, 1980).
14. Bocarsly, A. B., Tachikawa, H. & Faulkner, L. R. in *Laboratory Techniques in Electroanalytical Chemistry* 2nd edn (eds Kissinger, P. T. & Heineman, W. R.) 855–898 (Marcel Dekker, New York, 1996).
15. Trau, M., Saville, D. A. & Aksay, I. A. Field-induced layering of colloidal crystals. *Science* **272,** 706–709 (1996).
16. Böhmer, M. In situ observation of 2-dimensional clustering during electrophoretic deposition. *Langmuir* **12,** 5747–5750 (1996).
17. Trau, M., Saville, D. A. & Aksay, I. A. Assembly of colloidal crystals at electrode interfaces. *Langmuir* **13,** 6375–6381 (1997).
18. Richetti, P., Prost, J. & Barois, P. Two-dimensional aggregation and crystallization of a colloidal suspension of latex spheres. *J. Phys. Lett.* **45,** 1137–1143 (1984).
19. Richetti, P., Prost, J. & Barois, P. in *Physics of Complex and Supermolecular Fluids* (eds Safran, S. A. & Clark, N. A.) 387–411 (Wiley, New York, 1987).
20. Giersig, M. & Mulvaney, P. Formation of ordered 2-dimensional gold colloid lattices by electrophoretic deposition. *J. Phys. Chem.* **97,** 6334–6336 (1993).

21. Giersig, M. & Mulvaney, P. Preparation of ordered colloid monolayers by electrophoretic deposition. *Langmuir* **9,** 3408–3413 (1993).
22. Solomentsev, Y., Böhmer, M. & Anderson, J. L. Particle clustering and pattern formation during electrophoretic deposition: A hydrodynamic model. *Langmuir* **13,** 6058–6068 (1997).
23. Russel, W. B., Saville, D. A. & Schowalter, W. R. *Colloidal Dispersions* (Cambridge Univ. Press, Cambridge, UK, 1989).
24. van den Meerakker, J. E. A. M., Meulenkap, E. A. & Scholten, M. (Photo)electrochemical characterization of tin-doped indium oxide. *J. Appl. Phys.* **74,** 3282–3288 (1993).
25. Benkhelifa, F., Ashrit, P. V., Bader, G., Girouard, F. E. & Truong, V.-V. Near room temperature deposited indium tin oxide films as transparent conductors and counterelectrodes in electrochromic systems. *Thin Solid Films* **232,** 83–86 (1993).
26. Murali, K. R. *et al.* Characterization of indium tin oxide films. *Surf. Coatings Technol.* **35,** 207–213 (1988).

Acknowledgements

We thank Y. Xiao and H. F. Poon for assistance in the experimental work, and A. B. Bocarsly for discussions about semiconductor properties. This work was supported by a MURI grant from the US Army Research Office, NASA (Microgravity Science and Applications Division), and a MRSEC program of the NSF.

Correspondence and requests for materials should be addressed to I.A.A. (e-mail: iaksay@princeton.edu).

Shape control of CdSe nanocrystals

Xiaogang Peng*, Liberato Manna, Weidong Yang, Juanita Wickham, Erik Scher, Andreas Kadavanich & A. P. Alivisatos

Department of Chemistry, University of California at Berkeley, and Lawrence Berkeley National Laboratory, Berkeley, California 94720, USA

Nanometre-size inorganic dots, tubes and wires exhibit a wide range of electrical and optical properties[1,2] that depend sensitively on both size and shape[3,4], and are of both fundamental and technological interest. In contrast to the syntheses of zero-dimensional systems, existing preparations of one-dimensional systems often yield networks of tubes or rods which are difficult to separate[5–12]. And, in the case of optically active II–VI and III–V semiconductors, the resulting rod diameters are too large to exhibit quantum confinement effects[6,8–10]. Thus, except for some metal nanocrystals[13], there are no methods of preparation that yield soluble and monodisperse particles that are quantum-confined in two of their dimensions. For semiconductors, a benchmark preparation is the growth of nearly spherical II–VI and III–V nanocrystals by injection of precursor molecules into a hot surfactant[14,15]. Here we demonstrate that control of the growth kinetics of the II–VI semiconductor cadmium selenide can be used to vary the shapes of the resulting particles from a nearly spherical morphology to a rod-like one, with aspect ratios as large as ten to one. This method should be useful, not only for testing theories of quantum confinement, but also for obtaining particles with spectroscopic properties that could prove advantageous in biological labelling experiments[16,17] and as chromophores in light-emitting diodes[18,19].

The general preparation of spherical nanocrystals involves monitoring and manipulating the kinetics of their growth. In the case of cadmium selenide, CdSe, dimethylcadmium and selenium powder are co-dissolved in a tri-alkyl phosphine (-butyl or -octyl), and the solution injected into hot (340–360 °C), technical grade (90% purity) trioctyl phosphine oxide (TOPO)[14,15]. Nucleation occurs rapidly, followed by growth (280–300 °C). At the growth temperature, surfactant molecules adsorb and desorb rapidly from the nanocrystal surface, enabling the addition (as well as removal) of atoms from the crystallites, while aggregation is suppressed by the presence of (on average) one monolayer of surfactant at the crystallite surface.

Kinetic control is then used to manipulate the average particle size and size distribution. In earlier work[14], we showed that the growth process could occur in two different modes, depending upon the concentration of the monomer present: "focusing" of the size distribution, and "defocusing". During the focusing stage, the concentration of monomer in solution is higher than the solubilities

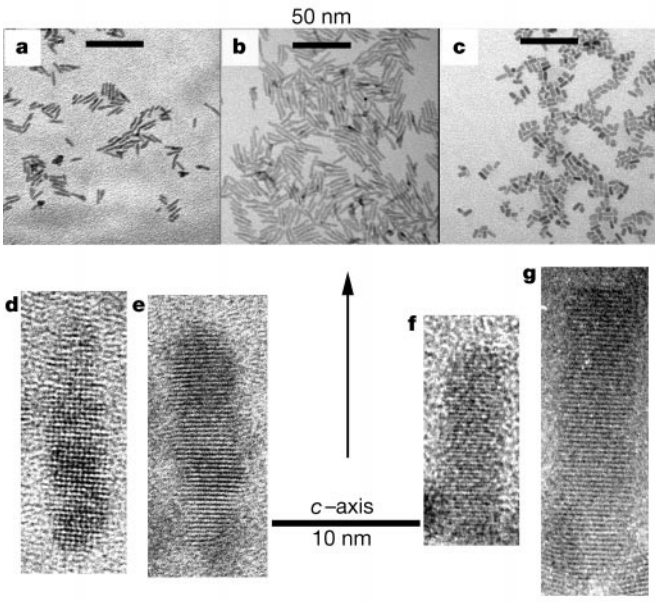

Figure 1 TEM images of different samples of quantum rods. **a–c,** Low-resolution TEM images of three quantum-rod samples with different sizes and aspect ratios. **d–g**, High-resolution TEM images of four representative quantum rods. **d** and **e** are from the sample shown in **a**; **f** and **g** are from the sample shown in **c**.

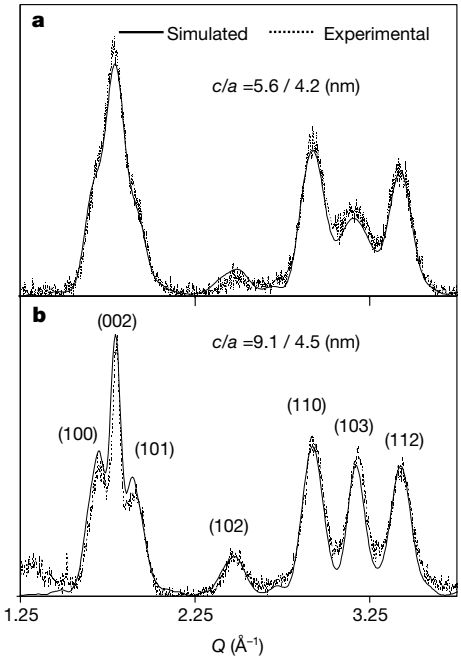

Figure 2 X-ray diffraction patterns of two CdSe rod-shaped nanocrystals. These two nanocrystals have the same short-axis dimension (within experimental error). The sizes and aspect ratios were found from the experimental patterns by the simulations shown.

* Present address: Department of Chemistry and Biochemistry, University of Arkansas, Fayetteville, Arkansas 727033, USA.